Kinesin Tail Domains and Mg^{2+} Directly Inhibit Release of ADP from Head Domains in the Absence of Microtubules[†]

David D. Hackney* and Maryanne F. Stock

Department of Biological Sciences, Carnegie Mellon University, Pittsburgh, Pennsylvania 15213

Received April 15, 2008; Revised Manuscript Received May 29, 2008

ABSTRACT: Kinesin-1 is a vesicle motor that can fold into a compact inhibited conformation that is produced by interaction of the heavy chain C-terminal tail region with the N-terminal motor domains (heads). Binding of the tail domains to the heads inhibits net microtubule-stimulated ATPase activity by blocking the ability of the heads to bind to microtubules with coupled acceleration of ADP release. We now show that folding of kinesin-1 also directly inhibits ADP release even in the absence of microtubules. With long heavy chain constructs such as DKH960 that exhibit a high degree of regulation by folding, the basal rate of ADP release is inhibited up to 30-fold compared to that of truncated DKH894 which has lost the inhibitory tail domains and does not fold. Inhibition of ADP release is also observed when separate head and tail domain constructs are mixed at low salt concentrations. This inhibition of ADP release by tail domains is formally analogous to the action of nucleotide dissociation inhibitors (NDI or GDI) for regulatory GTPases. In contrast to their inhibition of ADP release, tail domains accelerate the rate of ADP binding to nucleotide-free kinesin-1. Inhibition of release of ADP by tail domains is reversed by Unc-76 (FEZ1) which is a potential regulator of kinesin-1. Tail domains only weakly inhibit the initial slow release of Mg^{2+} from the kinesin−MgADP complex but strongly inhibit the fast release of Mg^{2+}-free ADP.

Kinesin-1 (hereafter termed kinesin) is a heterotetramer composed of two heavy and two light chains. It is highly elongated at high ionic strengths with two motor (head) domains at the N-terminus of the heavy chains that are separated from the light chains and the C-terminal tail domains of the heavy chains by a long region of coiled coil (see refs *1* and *2*). Under physiological conditions, however, kinesin is folded into a more compact conformation (*3*) that is produced by the interaction of specific regions in the head/neck and the tail of the heavy chain (*4, 5*). Light chains are not required for either motility or folding into the compact conformation, but their presence in the native heterotetramer destabilizes the folded conformation (*3*) and decreases the MT[1] affinity (*6*). Long dimeric constructs such as DKH960 (*Drosophila* kinesin heavy chain residues 1−960) are folded and have a highly inhibited MT-stimulated ATPase rate (*7*), compared to shorter constructs such as DKH894 that lacks the tail domains required for folding. This suggests that the interaction of the head and tail domains in the folded conformation is responsible for the inhibition of MT-stimulated ATPase activity and thus would provide a mechanism for preventing free kinesin in the cell from wastefully hydrolyzing ATP. Compared to other kinesin-1 species, the tail regions of fungal kinesin-1 species are not well conserved and they likely have a different mechanism of regulation (see ref *2*).

This simple interpretation, however, is complicated by the properties of the intermediate-length constructs DKH937 and DKH945 that also fold but are superactivated for bimolecular MT-stimulated ATPase activity to rates greater than for free heads alone, rather than inhibited (*7*). Superactivation is likely related to a strong MT-binding site in the tail that becomes unmasked in these partially truncated constructs and results in their greatly increased net affinity for MTs. Superactivated DKH937 and DKH945 lack all or part of the highly conserved IAK region (*4*), whereas the IAK region is intact in inhibited DKH960. This suggests that the IAK region is responsible for the inhibition that is observed in DKH960. Inhibition of the MT-stimulated activity of folded DKH960 is due to blocking of the initial binding of the heads to the MT with coupled release of bound ADP (*7*). The observation by Friedman and Vale (*8*) that folded kinesin has a greatly reduced rate of productive attachment to MTs leading to processive motion is consistent with this mechanism. Regulation of kinesin activity and cargo binding and unbinding in the cell is likely to be a complex process that involves a number of additional factors. Understanding the detailed mechanism of autoinhibition by tail domains will be an important initial step in laying the foundation on which other factors operate.

We report here that the binding of tail domains to heads also directly inhibits the basal rate of ADP release in the absence of MTs. This does not preclude an additional role for steric blocking in the MT-stimulated reaction in which tail domains would block productive association of the heads with the MT, but it does demonstrate that one factor in net

[†] This work supported by National Institutes of Health Grant NS25980 and National Science Foundation Grant 0615549.

* To whom correspondence should be addressed: Department of Biological Sciences, Carnegie Mellon University, 4400 Fifth Ave., Pittsburgh, PA 15213. Telephone: (412) 268-3244. Fax: (412) 268-7129. E-mail: ddh@andrew.cmu.edu.

[1] Abbreviations: MT, microtubule; mantADP, 2′(3′)-*O*-(*N*-methylanthraniloyl)adenosine 5′-diphosphate.

10.1021/bi8006687 CCC: $40.75
Published on Web 06/26/2008

inhibition is that tail domains thermodynamically favor a closed conformation with an inhibited rate of ADP release. Furthermore, separately expressed tail domains bind to head domains with inhibition of ADP release. This intermolecular interaction allows the energetics and kinetics of the binding of tails to head to be studied without the limitation of them being able to interact only intramolecularly in a full-length kinesin. It is shown that tail domains actually accelerate the rate of binding of ADP to kinesin and that tail domains preferentially bind to kinesin when ADP is also bound.

Analysis of the intermolecular interaction of tails and heads also provides a means of studying the effects of other molecules such as Mg^{2+} and Unc-76 that can influence the interaction of head domains with tail domains and ADP. Net release of MgADP from kinesin in the absence of MTs occurs by coupled slow release of both Mg^{2+} and ADP at high levels of Mg^{2+} or by sequential release of first Mg^{2+} followed by release of ADP at low concentrations of Mg^{2+} (*9*). For the sequential pathway, we show here that tail domains or Mg^{2+} strongly inhibit release of Mg-free ADP, but tail domains only weakly inhibit initial Mg^{2+} dissociation. Unc-76 from *Caenorhabditis elegans* and *Drosophila* and their mammalian homologues FEZ1 and FEZ2 play a role in regulation of transport (*10–12*) and bind directly to the kinesin tail in the region that also interacts with the heads to produce the folded state (*12–14*). Binding of FEZ alone is not sufficient to activate nucleotide-dependent binding of tetrameric kinesin in permeabilized cells without additional binding of the light chain cargo JIP1 to the light chains (*13*). We show here that Unc-76 alone, however, is sufficient for reversal of the inhibition of ADP release produced by tail domains in a reconstituted system in the absence of MTs and light chains.

MATERIALS AND METHODS

Kinesin constructs designated DKHxxx contain amino acid residues 1−*xxx* of conventional *Drosophila* kinesin (*15*), and they were expressed and purified as previously described (*4, 7, 16*). DKH952 is an additional construct that contains a stop codon after alanine 952, and DKH960HT has a GSHHHHHH sequence appended after alanine 960. DHK412 terminates at residue 412 and contains an additional TSHHHHHH sequence. Most experiments were performed with DKH412 as a model short dimer of head domains, but some experiments used DKH405 (*17*) that has similar properties. SC899−952 is a fusion of the stable coiled coil of GCN4-p1 (*18*) to residues 899−952 of the kinesin heavy chain. The N-terminal sequence appended to GCN4-p1 is MGSSHHHHHHRMKQL... with the start of GCN4-p1 underlined. The C-terminus of GCN4-p1 was fused to kinesin by substitution of the terminal arginine of GCN4-p1 by L899 of kinesin. The additional residues T and S were appended after alanine 952 of kinesin to incorporate a *Spe*I restriction site. SC899−940, SC899−927, and SC899−910 are identical except they terminate at kinesin residues 940, 927, and 910, respectively. TV-Unc76C is the C-terminal region (residues 254−474) of *Drosophila* Unc76 (*12*) expressed as a fusion protein with thioredoxin in pET32 whose thrombin cleavage site was converted into a TEV protease site. Proteins containing a His tag were purified by chromatography on NTA-Ni with elution by imidazole.

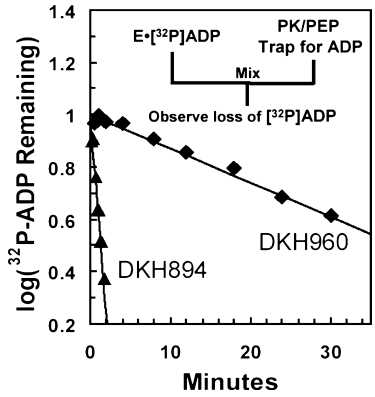

FIGURE 1: Release of [^{32}P]ADP by kinesin. Kinesin was equilibrated with [α-^{32}P]ATP to label the bound ADP, and then the reaction was initiated by dilution into A25 buffer containing 2 mM phosphoenolpyruvate, 1 mM MgATP, pyruvate kinase, and no added KCl. The reaction was quenched with HCl, and then the amount of pyruvate kinase-inaccessible [^{32}P]ADP was determined by anion exchange chromatography essentially as previously described (*19*): DKH894 (▲) and DKH960 (◆).

Nucleotide-free kinesin was prepared by chromatography on phosphocellulose in the presence of excess EDTA which greatly reduces the affinity for ADP (*9, 19*). All operations were performed at 4 °C in AE buffer (25 mM ACES {2-[(2-amino-2-oxoethyl)amino]ethanesulfonic acid}/KOH (pH 6.9) and 1 mM K-EDTA) with 2 mM dithiothreitol. After kinesin had been loaded onto phosphocellulose, the column was washed extensively with AE buffer containing 75 mM NaCl and 30% glycerol. ADP is rapidly eluted under these conditions, and washing was continued until the absorbance at 260 nn was indistinguishable from baseline. Kinesin was then eluted by increasing the concentration of NaCl to 800 mM.

All reactions were conducted at 25 °C in A25 buffer [25 mM ACES/KOH (pH 6.9), 2 mM magnesium acetate, 2 mM potassium EGTA, 0.1 mM potassium EDTA, and 1 mM 2-mercaptoethanol] supplemented with KCl where indicated. The free Mg^{2+} concentration in A25 buffer is approximately 1.9 mM (2 mM magnesium acetate minus 0.1 mM complexed with EDTA). ADP and ATP were added with equal molar levels of Mg^{2+} unless specifically indicated as Mg-free. The release of [^{32}P]ADP from kinesin was assessed essentially as previously described (*19*). The binding and release of mantADP were assessed by fluorescence with excitation at 285 nm to monitor FRET from kinesin tyrosines to the mant group of bound mantADP as previously described (*9, 20*). Error bars indicate the standard deviation.

RESULTS

Dependence of ADP Release Rate on Folding of Long Kinesins. As indicated in Figure 1, [^{32}P]ADP is released in a first-order process from unfolded DKH894 at 0.015 s^{-1} in A25 buffer (contains ∼1.9 mM free Mg^{2+}) without added KCl, and this value is typical of uninhibited kinesin head dimers (see refs *9* and *17*). Folded DKH960, however, has a 30-fold lower rate of ADP release at 0.00048 s^{-1}. Thus, interaction of tail domains with heads in folded DKH960 not only inhibits MT-stimulated ADP release as previously shown (*7*) but also inhibits the basal release of ADP in the absence of MTs. The results of similar analyses with a range of constructs and KCl concentrations are summarized in

Table 1: Influence of KCl on Basal ADP Release[a]

construct	rate (×10 s^{-1}(*3*)) 0 mM KCl	25 mM KCl	200 mM KCl	450 mM KCl	800 mM KCl
DKH365[b]	10.2	5.2	8.7	16.4	32
DKH405	−	9.8[c]	−	−	−
DKH894	14.9	7.4	−	17.0	23
DKH927	18.9	−	−	−	−
DKH937	6.0	−	−	−	−
DKH945	2.4	2.7	−	13.2	−
DKH952	0.50	0.95	−	−	12.9
DKH960-HT	−	1.06	−	−	−
DKH960	0.48	0.94	1.5	3.0	11.3

[a] Rate of [^{32}P]ADP release was determined as in Figure 1 with varying KCl concentrations. Missing values were not determined. [b] MantADP release from ref *37*. [c] From ref *17*.

Table 1. In 0 or 25 mM KCl, DKH927 and shorter constructs (*4*) are unfolded, and they all have uninhibited rates of 0.010−0.019 s^{-1}. DKH937 and DKH945 are folded at ≤25 mM KCl (*4*), and their truncated tail domains are therefore still in contact with the heads. These truncations produce a progressively decreasing level of inhibition of basal ADP release, but DKH937 and DKH945 in the absence of added KCl are still 60 and 84% inhibited, respectively, relative to unfolded DKH894. Although the inhibition of ADP release in folded DKH960 is incomplete, it is still greater than 50%, indicating that release of ADP from both heads is inhibited in the folded state. Short dimeric head constructs release both ADP molecules in a single first-order process (*21*), and this is also true for the long heavy chain constructs studied here even when they are folded (Figure 1 and additional data not shown). Thus, in the folded state, the two head domains have the same inhibited rate of ADP release, or if nonequivalent conformations with different ADP release rates exist, they must interconvert faster than the slow rate of ADP release so that only the average rate is observed.

Monomeric DKH365 has a minimum in its rate of ADP release at approximately 25 mM KCl, with increasing values at both lower and higher salt concentrations as determined previously (*9*) and included in Table 1 for comparison. Unfolded DKH894 has a similar pattern of salt dependence as seen in Table 1. The change in sedimentation coefficient with salt for DKH960 (*4*) indicates that it should still be mainly folded at 200 mM KCl but will shift to predominantly unfolded at 800 mM salt. At 200 mM KCl, DKH960 is still highly inhibited, consistent with a predominately folded state, but inhibition is increasingly lost at higher salt. At 450 mM KCl, the level of inhibition is reduced, but still substantial, whereas at 800 mM NaCl, the rate of release of ADP by DKH894 is only twice as fast as for DKH960. Because DKH945 unfolds at lower salt concentrations, it should be largely unfolded at 450 mM KCl (*4*) and its rate of ADP release in 450 mM salt is essentially uninhibited when compared to that of DKH894.

Table 1 includes results with two new constructs, DKH952 and DKH960HT, that were not available for the previous study of the dependence of MT activation on truncation position (*7*). DKH952 is truncated immediately following the highly conserved IAK region (*4, 7*), and DKH960HT contains a histidine tag of six histidine residues appended following residue 960. The folding of these constructs is similar to that of DKH960 in that they are both still largely folded at 300 mM salt but unfold at 1000 mM salt with $s_{20,w}$ values of ∼6.8 and ∼5.4 S at 300 and 1000 mM salt, respectively (not shown). The basal rates of release of ADP by these two constructs at 25 mM KCl (Table 1) are essentially identical to that for DKH960, consistent with their tight folding and inclusion of the full tail region needed for inhibition in the absence of MTs. When purified by gel filtration at 300 mM NaCl to remove aggregates and proteolysis fragments as described for DKH960 (*7*), they have bimolecular rates for MT-stimulated ATPase activity of 0.161 ± 0.003 and 0.708 ± 0.017 μM^{-1} s^{-1} for DKH952 and DKH960HT, respectively at 50 mM KCl. Thus, the inhibition of DKH952 is severe and similar to that of DKH960, the ATPase rate of which is 0.107 μM^{-1} s^{-1} under the same conditions (*7*). It is interesting to note that DKH945 which is only seven residues shorter than DKH952 has a MT-stimulated ATPase rate that is >1000-fold greater at 177 μM^{-1} s^{-1} (*7*). DKH960HT, however, is only partially inhibited with a rate intermediate between the value for DKH960 and the uninhibited rate of 15.4 μM^{-1} s^{-1} for DKH894 (*7*).

Inhibition of Basal MgADP Release by Separate Tail Domains in the Absence of MTs. The long kinesin constructs described above provide information about the properties of the folded state, but unfolding can be induced by truncation or by addition of high salt concentrations. Consequently, the detailed nature of the reversible interaction of head and tail domains in long constructs cannot be studied under more physiological conditions. Separately expressed dimeric head domains (DHK412 and DKH405) and a dimeric tail construct (SC899−952) were therefore used to study their reversible intermolecular interaction at lower ionic strengths. SC899−952 contains the stable coiled coil of GCN4 (*18*) fused to residues 899−952 of the kinesin heavy chain. This construct was used as a model for the tail of kinesin because it contains the full region required for interaction with the head region and because it is dimeric (N. Baek and D. D. Hackney, unpublished observations), whereas this region of kinesin is monomeric without fusion to GCN4. An anchored dimeric coiled coil tail construct is an appropriate model for the native interaction because it presents dimeric tails to the dimeric heads (intermolecularly in trans) in the same stoichiometry and orientation (the two tail peptides fused to the same end of a parallel coiled coil) which results from folding of full-length heavy chain dimers (intramolecularly in cis). Concentrations of heads, tails, and Unc-76 are given on a per polypeptide basis to conform to previous usage (*17*) and to avoid having to specify the oligomeric state which may not be known in all cases. Note, however, that because SC899−952 is likely dimeric in these experiments, the apparent K_d values for SC899−952 as a dimer would be half the values reported here on a monomer basis.

SC899−952 is a potent inhibitor of basal release of mantADP by dimeric DKH412 as indicated in Figure 2A. MantADP provides a useful fluorescence signal for following nucleotide binding because its kinetics of interactions with kinesin are similar to those of unmodified ADP. In the absence of SC899−952 (trace a), the fluorescence decreases in a first-order process as mantADP is released from the complex with kinesin and FRET from the tyrosines of DHK412 to the mant group is lost. The release of mantADP is strongly inhibited by 1 μM SC899−952 (trace b), and little

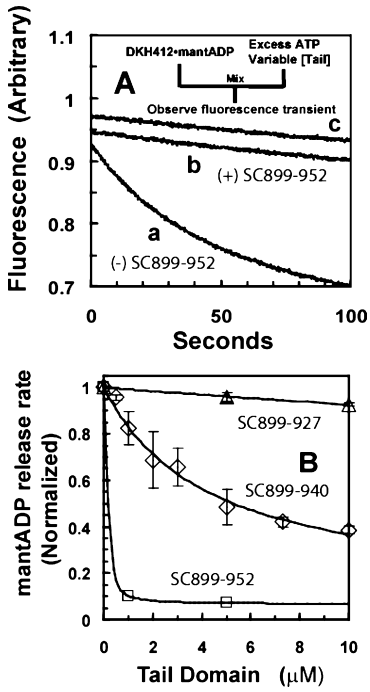

FIGURE 2: Inhibition by tail domains of release of mantADP from DKH412. (A) Time course of fluorescence change on mixing the DHK412−mantADP complex with excess ATP in A25 buffer without added KCl. Traces a, b, and c are with 0, 1, and 5 μM SC899−952, respectively. Final concentrations of 0.3 μM DKH412 and 200 μM ATP. (B) Dependence of the rate of release of mantADP on the concentration of tail domains with no added KCl. The DHK412−mantADP complex was mixed with excess ATP and tail domains: (□) SC899−952, (◇) SC899−940, and (△) SC899−927. Because the inhibited rates were too slow to determine a reliable first-order rate constant by fluorescence, the relative rates were approximated by using a linear fit to the curves between 5 and 20 s and then normalized to the rate in the absence of tail domains. Detailed fitting was not attempted for SC899−952 because the binding was too tight, but the inhibition appeared to saturate at ~92%. Conversely, the binding of SC899−927 was too weak to estimate an apparent K_d. The curve for SC899−940 was fit by nonlinear regression to a model in which the tail domain produced only partial inhibition of ADP release even when binding to heads was saturated. The fraction of heads with a tail bound was calculated using the full quadratic expression for mutual depletion (*38*) at a final DHK412 concentration of 0.3 μM. The fit for SC899−940 yielded a maximum inhibition of 89% and an apparent K_d of 4 μM.

additional inhibition is observed at 5 μM SC899−952 (trace c). Immediately after DHK412 with SC899−952 are mixed, mantADP should be released at the same rapid rate seen in the absence of SC899−952 (trace a), until mantADP release is inhibited by binding of SC899−952. The lack of a fast initial phase in traces b and c before the onset of inhibition indicates that the interaction of DHK412 and SC899−952 is rapid on this time scale. The shorter construct, SC889−940, has lost the IAK domain but still produces significant maximum inhibition of ADP release as shown in Figure 2B. This result is consistent with the reduced, but still significant, inhibition observed in Table 1 for DKH945 and DKH937 in the folded conformation at low KCl concentrations. However, the affinity of SC899−940 for DHK412 is weak without the IAK domain (apparent K_d of 4 μM for SC899−940 versus <0.1 μM for SC899−952). The decreased affinity of SC899−940 for DHK412 is consistent with the unfolding of DKH945 and DKH937 at

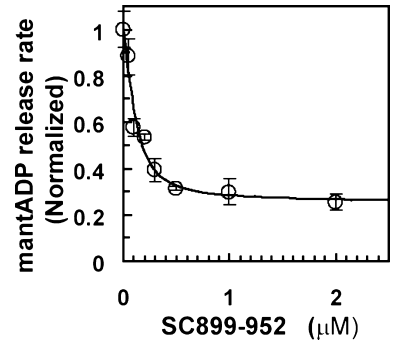

FIGURE 3: Inhibition by SC899−952 of mantADP release in 25 mM KCl. As in Figure 2, but with 25 mM KCl, 0.14 μM DHK412, and a variable concentration of SC899−952. The fit to a mutual depletion model yielded 75% maximum inhibition and an apparent K_d of 0.04 μM.

moderate ionic strengths, whereas DKH952 or DKH960 unfolds only at much higher ionic strengths (*4*). The shorter DKH927 and DKH910 remain unfolded even at low ionic strengths, and no significant inhibition of ADP release is observed with SC889−927 (Figure 2B) or SC899−910 (not shown), as expected if their interaction with heads is weak and potentially not inhibitory.

In Figure 2 without added KCl, the affinity of SC899−952 is too high for accurate determination of a dissociation constant due to mutual depletion. However, a higher ionic strength weakens the binding as indicated in Figure 3 in the presence of 25 mM KCl. The apparent K_d obtained from the fit is 0.04 μM but is not well defined because the K_d is still lower than the concentration of DHK412 (0.14 μM). In agreement with the results of Table 1, the intermolecular inhibition induced by separate tail domains in trans reproduces the pattern of inhibition seen intramolecularly for DKH952 and KDH960 with incomplete inhibition at saturation of binding and less maximal inhibition at 25 mM KCl versus 0 mM KCl.

Reversal of Inhibition by Unc-76. Unc-76 (FEZ1) is a regulator of kinesin activity whose C-terminal region binds to the kinesin tail in the same part of the tail that interacts with the heads to produce the folded state (*12, 13*). In permeabilized cells, Unc-76 requires the additional binding of the light chain cargo JIP1 to the light chains of the native heterotetramer to activate microtubule binding (*13*). The results of Figure 4, however, indicate that the C-terminal part of Unc-76 (TV-Unc-76C) alone is sufficient for reversal of the inhibition of mantADP release that is produced by SC899−952 in the absence of light chains. In this experiment, the DHK412−mantADP complex with or without SC899−952 was mixed with Unc-76 and excess ATP and the rate of release of mantADP determined. In the absence of SC899−952, Unc-76 has no systematic effect on the ADP release rate. A small excess of SC899−952 over DHK412 (0.5 and 0.3 μM, respectively) produces 86% inhibition in the absence of Unc-76, but increasing amounts of Unc-76 reverse the inhibition in a concentration-dependent manner. Heads and Unc-76 both bind to the same region of the tail (*12–14*), and this suggests that the relief of inhibition by Unc-76 is due to a competition in which Unc-76 can displace heads from tails. Detailed modeling under the conditions of Figure 4 is complicated by the tight binding of SC899−952 to both DKH412 and Unc-76 that requires

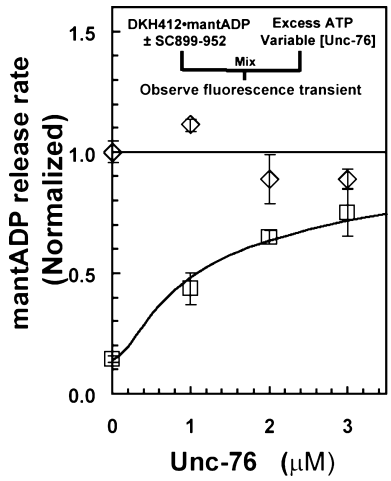

FIGURE 4: Relief of inhibition by Unc76. The DHK412−mantADP complex either in the presence or in the absence of SC899−952 was mixed in the stopped flow with ATP and variable Unc-76 levels. Final concentrations were as follows: 0.3 μM DHK412, 0 (◇) or 0.5 μM (□) SC899−952, 200 μM ATP, and Unc-76 as indicated.

mutual depletion of both be considered. The curve indicated in Figure 4 was obtained by simulation using a competitive model with full mutual depletion and K_d values of 0.01 and 0.03 μM for binding of SC899−952 to DKH412 and Unc-76, respectively. However, other K_d values yield similar agreement with the experimental points as long as binding remains tight and the binding of SC899−952 to Unc-76 is ~3-fold weaker than that to DKH412.

Influence of SC899−952 on ADP Binding by Nucleotide-Free Heads. Drosophila kinesin is unstable in the absence of nucleotide (*22*), but nucleotide-free kinesin can be prepared if it is stabilized by high concentrations of glycerol and NaCl as reported by Ma and Taylor (*23*). To minimize inactivation during mantADP binding experiments at lower salt concentrations, a concentrated stock of stabilized nucleotide-free DKH405 was diluted into A25 buffer at 25 °C with 25 mM KCl and 20% sucrose and then mixed in the stopped flow with mantADP (without sucrose) after a variable delay. Figure 5A gives representative traces for the increase in fluorescence accompanying binding of mantADP after different aging periods in the absence of SC899−952. Binding of mantADP to nucleotide-free head domains can produce a complex transient with an overshoot at high nucleotide concentrations due to a two-step binding reaction (*23*) but obeys simple first-order kinetics at the low mantADP concentration of 2 μM employed here. The amplitudes of the transients decrease with an increase in the length of incubation due to conversion of nucleotide-free DHK405 to the inactive conformation that cannot bind mantADP. A plot of the log of the amplitude change versus time of incubation (Figure 5A, inset) yields a first-order rate constant for inactivation of 6.1×10^{-3} s^{-1}. Without the 20% sucrose in the incubation, DHK405 is largely inactivated in the time required to load and prime the stopped flow. The observed first-order rate for mantADP binding remains approximately constant until the amplitude becomes too small for accurate measurement, consistent with nucleotide binding only to active heads whose concentration falls with time. For aging times of less than 180 s, the average rate was 7.26 ± 0.39

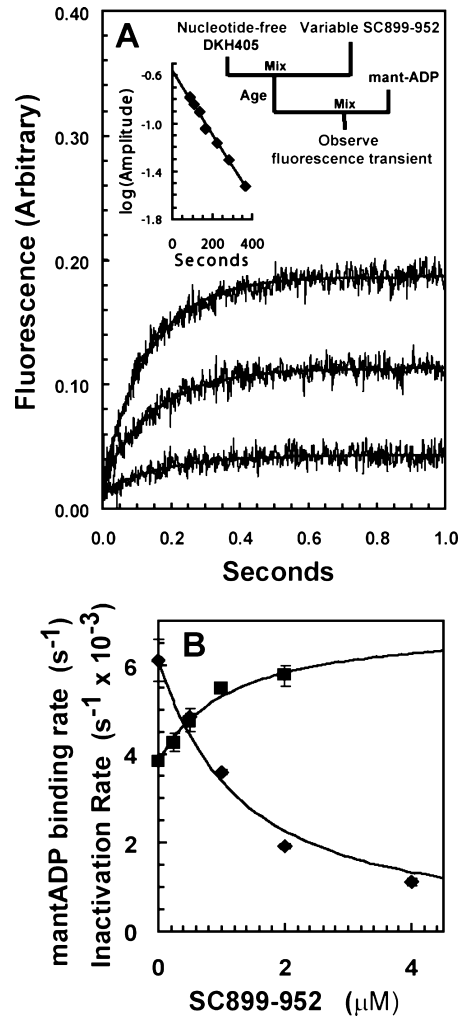

FIGURE 5: Binding of mantADP to nucleotide-free DKH405. Nucleotide-free DKH405 was diluted to 0.4 μM in A25 buffer with 25 mM KCl, 20% sucrose, and variable concentrations of SC899−952 to initiate the reaction. The diluted DKH405 was then aged for 1−5 min before being mixed with an equal volume of 4 μM mantADP in the stopped flow for observation of the fluorescence transient that occurred on mantADP binding. Final concentrations during the mantADP binding transient were as follows: 0.2 μM DKH405, 2 μM mantADP, and 10% sucrose. (A) Representative fluorescence transients in the absence of tail domains after incubation for 88, 165, and 300 s (from top to bottom trace) before mixing with mantADP. First-order fits to the transients are indicated by the smooth lines. The rate of decrease of the amplitudes follows first-order kinetics with a rate constant of 6.1×10^{-3} s^{-1} as indicated in the inset (includes other time points whose transients are not plotted in the main figure for clarity). (B) Summary of the influence of SC899−952 on the rates of inactivation and ADP binding. Experiments were performed as described for panel A, but with SC899−952 present during the aging period, and the results are summarized. For analysis of inactivation (◆), the rates of inactivation at different concentrations of SC899−952 were fit to a mutual depletion model using the concentrations of DKH405 and SC899−952 during the aging period. The fit yielded an apparent K_d of 1.03 μM and complete protection from inactivation at saturation with SC899−952. For binding of mantADP (■), the bimolecular rate constants for mantADP binding at different concentrations of SC899−952 were also fit to a mutual depletion model, but using the lower concentrations of SC899−952 and DKH405 present during the mantADP binding reaction (after mixing with an equal volume of a solution containing mantADP). The fit yielded an apparent K_d of 0.97 μM and a maximum rate of 6.8 s^{-1}.

s^{-1}. This corresponds to a bimolecular rate for mantADP binding of 3.8 μM^{-1} s^{-1} at an average mantADP concentration of 1.9 μM under these approximately pseudo-first-order conditions (10-fold excess of mantADP over DKH405).

Inclusion of SC899−952 in the incubation before mixing with mantADP stabilizes DHK405 against inactivation as indicated in Figure 5B, with the inactivation rate falling from 6.1×10^{-3} s^{-1} in the absence of SC899−952 to 1.1×10^{-3} s^{-1} with 4 μM SC899−952. In contrast to the inhibition of ADP release produced by binding of tail domains, binding of SC899−952 to nucleotide-free DHK405 actually increases the rate of binding of mantADP from 3.8 to >6 μM^{-1} s^{-1}. Both the dependence of the rate of inactivation and the increase in the rate of mantADP binding are consistent with binding of SC899−952 to nucleotide-free K405 with an apparent K_d of approximately 1 μM.

Inhibition by SC899−952 of Initial Mg^{2+} Release in the Sequential Pathway. Previous work (*9*) established that net release of MgADP in part occurred via a sequential pathway with initial slow release of Mg^{2+}, followed by rapid release of Mg-free ADP. This was based on two observations. One was that release of ADP from the complex of kinesin with Mg-free ADP was fast (complete within the time required for manual mixing). The other was that the net rate of release of ADP from the complex of kinesin with MgADP was accelerated by the presence of EDTA to trap any Mg^{2+} that was released. This was consistent with release of Mg^{2+} being faster than release of MgADP or ADP alone. In the presence of an EDTA trap, initial release of Mg^{2+} is irreversible and followed by rapid release of ADP. Free Mg^{2+} could suppress this pathway by rebinding to the kinesin−ADP complex before ADP could be released. In agreement with these previous results with monomeric DKH365 (*9*), excess EDTA as a Mg trap accelerates the net rate of MgADP release with dimeric DHK412 from typically ~0.01 s^{-1} in A25 buffer (contains 1.9 mM free Mg^{2+}) with 25 mM KCl to 0.036 s^{-1} in AE buffer (1 mM EDTA) with 25 mM KCl as indicated in Figure 6, trace a. SC899−952 does inhibit the net rate with a Mg trap (Figure 6, trace b), but only modestly with a maximum level of 36% inhibition (Figure 6, inset). The inhibition saturates at very low SC899−952 concentrations, in agreement with the tight binding observed in Figure 3.

Inhibition by SC899−952 of Release of Mg-Free ADP. The stopped flow results of Figure 7 (trace a) confirm that release of Mg-free ADP is fast and provide a value of 18.4 ± 0.6 s^{-1} for the rate. Furthermore, inclusion of 1.9 mM free Mg^{2+} in the chase blocks the rapid release of Mg-free ADP as indicated by trace d in Figure 7. This is consistent with millimolar levels of free Mg^{2+} being able to bind to the kinesin−Mg-free ADP complex to re-form the slowly releasing kinesin−MgADP complex, before ADP can be released from the Mg-free complex at 18 s^{-1}. The release of Mg-free ADP is strongly inhibited by binding of SC899−952 (traces b and c) with a decrease from 18.4 s^{-1} in the absence of SC899−952 to 3.0 ± 0.1 s^{-1} at both 1 and 2 μM SC899−952.

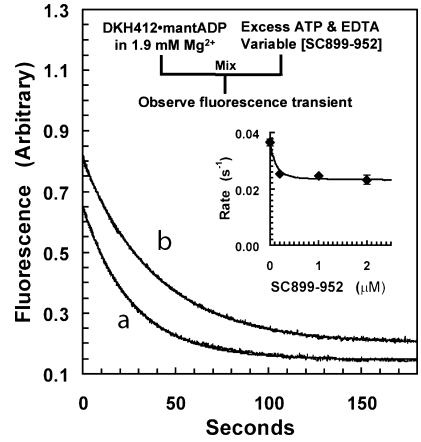

FIGURE 6: Inhibition by SC899−952 of net release of MgADP in the presence of a Mg^{2+} trap. A concentrated stock of kinesin as the complex with Mg-mantADP in A25 buffer was diluted into AE buffer with excess EDTA, 25 mM KCl, and excess ADP, and the fluorescence transient accompanying net release of mantADP was observed. Traces a and b are with 0.14 μM DHK412 with 0 and 0.2 μM SC899−952, respectively. Smooth lines are first-order fits at 0.037 and 0.025 s^{-1}, respectively. The inset gives the observed rate vs the concentration of SC899−952. The theoretical line in the inset is a fit to a mutual depletion model with the K_d held at the value of 0.04 μM seen in A25 buffer with 25 mM KCl in Figure 3 and the maximum inhibition varied to obtain a limiting value of 0.023 s^{-1} at saturation with SC899−952.

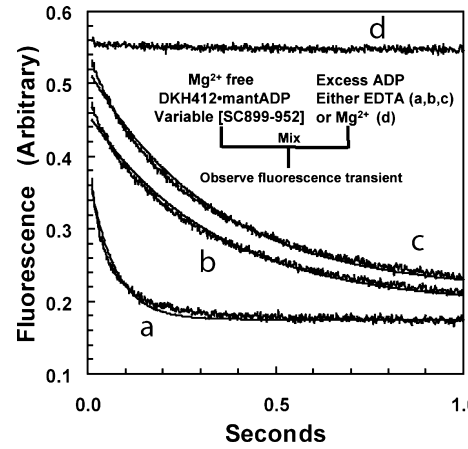

FIGURE 7: Inhibition by SC899−952 of release of Mg-free ADP from kinesin. The complex of kinesin with Mg-free mantADP was generated in the absence of significant free Mg^{2+} by dilution of a concentrated stock of the kinesin−Mg−mantADP complex into AE buffer (contains 1 mM EDTA and no magnesium) with 25 mM KCl and 20% sucrose. After the sample had been aged for 3 min to allow release of Mg^{2+} and trapped by the excess EDTA, a variable amount of SC899−952 was added and then mixed in the stopped flow with AE buffer containing 25 mM KCl and a chase of excess Mg-free ADP. All traces are at 0.7 μM DKH412. For traces a−c, SC899−952 was included in the chase for final SC899−952 concentrations of 0, 1, and 2 μM, respectively. Traces a−c show small deviations from a simple first-order process, and the source of this apparent heterogeneity is not known. Trace d was in the absence of SC899−952, but with the EDTA chase buffer replaced with A25 buffer (which contains 1.9 mM free Mg^{2+}) and 25 mM KCl.

DISCUSSION

Most current views of the mechanism of stimulation of motor proteins by actin or MTs involve switching between a closed state with tight nucleotide binding and an open state with rapid nucleotide release (*24, 25*). Although X-ray crystallography has proven to be ambiguous in providing a detailed structural and energetic basis for the open−closed transition and its dependence on nucleotide and different definitions have been employed for the closed and open conformations, the structure in solution must be in a

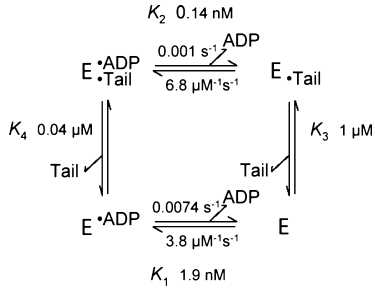

FIGURE 8: Scheme for thermodynamic coupling of ADP and tail binding.

conformation that is "closed" as defined by its inability to release ADP rapidly. In this context, the basal release of ADP from kinesin in the absence of MTs is slow because only a small fraction of the enzyme−ADP complex is present in an open conformation that is competent for rapid ADP release. Tail domains are shown here to stabilize the conformation with bound ADP and further reduce the already slow rate of ADP release. This mode of action is formally analogous to that of the nucleotide dissociation inhibitors (NDIs and GDIs) that bind to G-proteins and inhibit the release of GDP (*26–28*). The inhibition of ADP release by tails also provides a useful probe of the nature and energetics of the interaction of heads with tails that is difficult to obtain by other means.

Binding of tail domains and ADP to heads forms a closed thermodynamic cycle as indicated in Figure 8. The tighter binding of SC899−952 to heads when ADP is bound [$K_4 \sim 0.04$ μM (Figure 3)] than when ADP is not bound [$K_3 = 1$ μM (Figure 5)] requires that binding of SC899−952 cause a matching increase in the affinity for ADP. The K_d values for ADP can be calculated from the association and dissociation rate constants in the two cases. Typical values for release of ADP with 25 mM KCl from uninhibited heads and the head−tail complex are 0.0074 and 0.001 s^{-1}, respectively (Table 1), for DKH894 and DKH960. The measured bimolecular rate constants for ADP binding are 3.8 and 6.8 μM^{-1} s^{-1} (Figure 6). This gives calculated values of 1.9 and 0.14 nM for K_1 and K_2, respectively. The 14-fold change in ADP affinity (K_1/K_2) is in good agreement with the 25-fold shift in tail affinity (K_3/K_4) with allowance for the uncertainty in the estimation of K_4, small differences in ionic strength, and the presence of sucrose in some cases.

Interaction of kinesin with MTs shifts the open−closed equilibrium toward the open conformation and results in rapid net ADP release. By stabilizing the closed conformation, tail domains would also likely disfavor the MT-induced conversion to the open conformation and consequently inhibit MT-induced ADP dissociation as well. Direct comparison of the effect of tails on MT-stimulated versus basal ADP release, however, is not possible because the maximum rate of release of ADP from the quaternary complex of kinesin with MTs, tails, and ADP is not known. What is known is that tail domains strongly inhibit the net bimolecular $k_{bi(ADP)}$ rate for initial MT-stimulated ADP release by 80-fold [0.197 μM^{-1} s^{-1} for unfolded DKH894 vs 0.0025 μM^{-1} s^{-1} for folded DKH680 in 50 mM KCl (*7*)]. This net rate is equal to the maximum rate of ADP release at saturating MT levels divided by the K_d for binding of the kinesin−ADP complex to MTs. Tail domains could inhibit bimolecular MT-stimulated ADP release by affecting either or both of these components. Tails stabilize net ADP binding by 14-fold in the absence of MTs (Figure 8), and this would lower the rate of MT-stimulated ADP release by a corresponding amount if the stabilization by tails of the closed conformation had to be reversed upon formation of the MT-bound open conformation leading to ADP release.

Stabilization of bound ADP by tail domain interaction does not preclude additional roles for tail domains acting as a lid over the bound ADP or sterically blocking the binding of heads to MTs. Recent cross-linking studies are in fact consistent with interaction of the tail with the switch I region (*29*). The acceleration of ADP binding by tail domains, however, indicates that tail domains cannot also be serving as a lid in the ADP-free state because they would sterically block access by ADP and inhibit binding. In the absence of ADP, the tail domains must become disordered or relocate to a nonblocking conformation that favors ADP binding.

Significantly, the conserved IAK region is not required for inhibition of ADP release in the absence of MTs, as indicated by the partial inhibition still observed in folded conformations of DKH937 and DKH945 (Table 1) that lack part or all of the IAK domain and by the inhibition produced by SC899−940 (Figure 2B). The principal consequence of inclusion of the full IAK region in SC899−952 is to increase the affinity for heads and to increase the maximum extent of inhibition. This inhibition of basal ADP release for DKH937 and DKH940 is in stark contrast to the superactivation of their MT-stimulated ADP release (*7*). One factor that likely contributes to this difference is a region with five positive charges between residues 929 and 936 that adjoins the IAK region. Constructs that contain this positively charged region bind tightly to MTs when they are separately expressed (*5, 7, 30*), and the tail thus contains a nucleotide-independent auxiliary MT binding site (ABS) (*31*) in addition to the nucleotide-dependent MT binding of the heads. This ABS in the tail of kinesin is apparently masked in folded constructs that contain an intact IAK region but becomes exposed when the IAK region is disrupted as in DKH937 and DKH945. Thus, it remains to be determined how much of the increase in MT affinity produced by disruption of the IAK region is due to its direct role in inhibiting ADP release versus the increased net MT binding produced by unmasking the ABS or other interactions.

Tail domains have a greatly weakened effect on ADP release during the processive movement of kinesin following initial ADP release. Friedman and Vale (*8*) observed long, albeit discontinuous, processive runs with a folded construct. Folded DKH960 still has high kinetic processivity with more than 40 ATP molecules hydrolyzed per processive run as measured by its $k_{bi(Ratio)}$ value (*4*) and a high maximum ATPase rate at low salt concentrations in spite of its low rate of initial MT-stimulated ADP release. The ABS domain may play a role in prolonging processive runs. If the head−tail interaction needs to be disrupted for initial MT-stimulated ADP release to occur, then the binding of the exposed ABS domain to the MT could inhibit rebinding of the tail to the head domains.

Recent studies with several myosin family members have indicated that Mg^{2+} and ADP are not always released in a coupled manner and that control of initial Mg^{2+} release may be an important factor (*29, 32–34*). Switch I interacts with the bound Mg^{2+}, and selective movement of switch I provides

a potential mechanism for release of Mg^{2+} before release of ADP (see ref *35*). With kinesin at a low Mg^{2+} concentration in the absence of MTs or inhibition by tail domains, net release of MgADP occurs predominately by a sequential pathway with slow release of Mg^{2+} ($\sim$0.03 s^{-1}) followed by rapid release of Mg-free ADP at 18 s^{-1} as indicated by the results depicted in Figures 6 and 7. The rate for this sequential pathway will be the rate of release of Mg^{2+} ($\sim$0.03 s^{-1}) times the fraction of Mg-free ADP that is released from kinesin before rebinding of Mg^{2+} can occur. In the presence of excess EDTA, this fraction will be close to 1 because rebinding of Mg^{2+} to kinesin cannot occur and the maximum rate of 0.03 s^{-1} will be observed. Free Mg^{2+} at 1.9 mM reduces the fraction of the ADP that is released before Mg^{2+} rebinding occurs to essentially zero (no initial burst of ADP release before the onset of inhibition in Figure 7, trace d) and would produce a corresponding inhibition of the sequential pathway. However, net ADP release of $\sim$0.01 s^{-1} is still observed at 1.9 mM free Mg^{2+} in A25 buffer at low KCl concentrations (Table 1), and even much higher Mg^{2+} concentrations do not produce further inhibition of net ADP release (Figure 4b of ref *9*). This continued ADP release after essentially complete inhibition of the sequential pathway must therefore be occurring through a nonsequential pathway. SC899−952 strongly inhibits both release of MgADP by the nonsequential pathway (Figure 3) and release of Mg-free ADP (Figure 7) but is relatively ineffective in inhibition of the initial release of Mg^{2+} by the sequential pathway (Figure 6). Tail domains may in fact not inhibit initial Mg^{2+} release by the sequential pathway at all, because most, if not all, of the decrease in rate from 0.036 to 0.023 s^{-1} observed in the inset of Figure 6 for inhibition by SC899−952 in the presence of a Mg^{2+} trap can be ascribed to the expected strong inhibition of the nonsequential pathway (Figure 3) that is likely occurring in parallel at a rate of $\sim$0.01 s^{-1}.

For the uninhibited reaction in the absence of tail domains, removal of Mg^{2+} accelerates net ADP release by 1800-fold from $\sim$0.01 to 18 s^{-1}. Although the rate of initial release of Mg^{2+} from the MT complex is not known, it is interesting to note that if Mg^{2+} binding was disrupted, only an additional $\sim$10-fold further increase in the rate of ADP release would be needed to obtain the maximum MT-stimulated rate of $\sim$ 200 s^{-1} (see ref *36*). Thus disruption of the Mg^{2+} interactions on binding to MTs could produce a large acceleration in ADP release, but further changes would also be required to produce the full activation of ADP release that occurs on binding to MTs.

ACKNOWLEDGMENT

We thank Wei Jiang for preparation of nucleotide-free DKH405, Peter Kim for the CGN4-p1 plasmid, and Avin Snyder and Jessica Woessner for participation in cloning and protein purification.

REFERENCES

1. Hackney, D. D. (2007) Jump-starting kinesin. *J. Cell Biol. 176*, 7–9.
2. Adio, S., Reth, J., Bathe, F., and Woehlke, G. (2006) Review: Regulation mechanisms of kinesin-1. *J. Muscle Res. Cell Motil. 27*, 153–160.
3. Hackney, D. D., Levitt, J. D., and Suhan, J. (1992) Kinesin undergoes a 9 to 6 S conformational transition. *J. Biol. Chem. 267*, 8696–8701.
4. Stock, M. F., Guerrero, J., Cobb, B., Eggers, C. T., Huang, T.-G., Li, X., and Hackney, D. D. (1999) Formation of the compact conformer of kinesin requires a C-terminal heavy chain domain and inhibits microtubule-stimulated ATPase activity. *J. Biol. Chem. 274*, 14617–14623.
5. Yonekura, H., Nomura, A., Ozawa, H., Tatsu, Y., Yumoto, N., and Uyeda, T. Q. (2006) Mechanism of tail-mediated inhibition of kinesin activities studied using synthetic peptides. *Biochem. Biophys. Res. Commun. 343*, 420–427.
6. Verhey, K. J., Lizotte, D. L., Abramson, T., Barenboim, L., Schnapp, B. J., and Rapoport, T. A. (1998) Light chain-dependent regulation of kinesin's interaction with microtubules. *J. Cell Biol. 143*, 1053–1066.
7. Hackney, D. D., and Stock, M. F. (2000) Kinesin's IAK tail domain inhibits initial microtubule-stimulated ADP release. *Nat. Cell Biol. 2*, 257–260.
8. Friedman, D. S., and Vale, R. D. (1999) Single-molecule analysis of kinesin motility reveals regulation by the cargo-binding tail domain. *Nat. Cell Biol. 1*, 293–297.
9. Cheng, J. Q., Jiang, W., and Hackney, D. D. (1998) Interaction of mant-adenosine nucleotides and magnesium with kinesin. *Biochemistry 37*, 5288–5295.
10. Bloom, L., and Horvitz, H. R. (1997) The *Caenorhabditis elegans* gene unc-76 and its human homologs define a new gene family involved in axonal outgrowth and fasciculation. *Proc. Natl. Acad. Sci. U.S.A. 94*, 3414–3419.
11. Kuroda, S., Nakagawa, N., Tokunaga, C., Tatematsu, K., and Tanizawa, K. (1999) Mammalian homologue of the *Caenorhabditis elegans* UNC-76 protein involved in axonal outgrowth is a protein kinase C ζ-interacting protein. *J. Cell Biol. 144*, 403–411.
12. Gindhart, J. G., Chen, J., Faulkner, M., Gandhi, R., Doerner, K., Wisniewski, T., and Nandlestadt, A. (2003) The kinesin-associated protein UNC-76 is required for axonal transport in the *Drosophila* nervous system. *Mol. Biol. Cell 14*, 3356–3365.
13. Blasius, T. L., Cai, D., Jih, G. T., Toret, C. P., and Verhey, K. J. (2007) Two binding partners cooperate to activate the molecular motor kinesin-1. *J. Cell Biol. 176*, 11–17.
14. Fujita, T., Maturana, A. D., Ikuta, J., Hamada, J., Walchli, S., Suzuki, T., Sawa, H., Wooten, M. W., Okajima, T., Tatematsu, K., Tanizawa, K., and Kuroda, S. (2007) Axonal guidance protein FEZ1 associates with tubulin and kinesin motor protein to transport mitochondria in neurites of NGF-stimulated PC12 cells. *Biochem. Biophys. Res. Commun. 361*, 605–610.
15. Yang, J. T., Saxton, W. M., and Goldstein, L. S. (1988) Isolation and characterization of the gene encoding the heavy chain of *Drosophila* kinesin. *Proc. Natl. Acad. Sci. U.S.A. 85*, 1864–1868.
16. Stock, M. F., and Hackney, D. D. (2001) Expression of kinesin in *E. coli*. In *Methods in Molecular Biology: Kinesin Protocols* (Vernos, I., Ed.) pp 43−48, Humana Press, Totowa, NJ.
17. Jiang, W., Stock, M., Li, X., and Hackney, D. D. (1997) Influence of the kinesin neck domain on dimerization and ATPase kinetics. *J. Biol. Chem. 272*, 7626–7632.
18. Lumb, K. J., Carr, C. M., and Kim, P. S. (1994) Subdomain folding of the coiled coil leucine zipper from the bZIP transcriptional activator GCN4. *Biochemistry 33*, 7361–7367.
19. Hackney, D. D., Malik, A., and Wright, K. W. (1989) Nucleotide-free kinesin hydrolyzes ATP with burst kinetics. *J. Biol. Chem. 264*, 15943–15948.
20. Hackney, D. D. (2002) Pathway of ADP-stimulated ADP release and dissociation of tethered kinesin from microtubules. Implications for the extent of processivity. *Biochemistry 41*, 4437–4446.
21. Hackney, D. D. (1994) The rate limiting step in microtubule-stimulated ATP hydrolysis by dimeric kinesin head domains occurs while bound to the microtubule. *J. Biol. Chem. 269*, 16508–16511.
22. Huang, T.-G., and Hackney, D. D. (1994) *Drosophila* kinesin minimal motor domain expressed in *Escherichia coli*. Purification and kinetic characterization. *J. Biol. Chem. 269*, 16493–16501.
23. Ma, Y. Z., and Taylor, E. W. (1995) Kinetic mechanism of kinesin motor domain. *Biochemistry 34*, 13233–13241.
24. Kikkawa, M. (2008) The role of microtubules in processive kinesin movement. *Trends Cell Biol. 18*, 128–135.
25. Kull, F. J., and Endow, S. A. (2002) Kinesin: Switch I & II and the motor mechanism. *J. Cell Sci. 115*, 15–23.
26. Nuoffer, C., and Balch, W. E. (1994) GTPases: Multifunctional molecular switches regulating vesicular traffic. *Annu. Rev. Biochem. 63*, 949–990.
27. Grizot, S., Faure, J., Fieschi, F., Vignais, P. V., Dagher, M. C., and Pebay-Peyroula, E. (2001) Crystal structure of the Rac1-

RhoGDI complex involved in NADPH oxidase activation. *Biochemistry 40*, 10007–10013.
28. Kimple, R. J., Kimple, M. E., Betts, L., Sondek, J., and Siderovski, D. P. (2002) Structural determinants for GoLoco-induced inhibition of nucleotide release by Gα subunits. *Nature 416*, 878–881.
29. Rice, S. E., Dietrich, K. A., and Larson, A. G. (2008) Mechanisms of kinesin-1 regulation and coordination. *Biophys. J.* (Abstract Issue), 371.
30. Navone, F., Niclas, J., Hom-Booher, N., Sparks, L., Bernstein, H. D., McCaffrey, G., and Vale, R. D. (1992) Cloning and expression of a human kinesin heavy chain gene: Interaction of the COOH-terminal domain with cytoplasmic microtubules in transfected CV-1 cells. *J. Cell Biol. 117*, 1263–1275.
31. Stock, M. F., Chu, J., and Hackney, D. D. (2003) The kinesin family member BimC contains a second microtubule binding region attached to the N-terminus of the motor domain. *J. Biol. Chem. 278*, 52315–52322.
32. Hannemann, D. E., Cao, W., Olivares, A. O., Robblee, J. P., and De La Cruz, E. M. (2005) Magnesium, ADP, and actin binding linkage of myosin V: Evidence for multiple myosin V-ADP and actomyosin V-ADP states. *Biochemistry 44*, 8826–8840.
33. Rosenfeld, S. S., Houdusse, A., and Sweeney, H. L. (2005) Magnesium regulates ADP dissociation from myosin V. *J. Biol. Chem. 280*, 6072–6079.
34. Fujita-Becker, S., Durrwang, U., Erent, M., Clark, R. J., Geeves, M. A., and Manstein, D. J. (2005) Changes in Mg^{2+} ion concentration and heavy chain phosphorylation regulate the motor activity of a class I myosin. *J. Biol. Chem. 280*, 6064–6071.
35. Kull, F. J., and Endow, S. A. (2002) Kinesin: Switch I & II and the motor mechanism. *J. Cell Sci. 115*, 15–23.
36. Hackney, D. D. (2003) Motor proteins of the kinesin superfamily. *Enzymes (3rd Ed.) 23*, 88–143.
37. Jiang, W., and Hackney, D. D. (1997) Monomeric kinesin head domains hydrolyze multiple ATP molecules before release from a microtubule. *J. Biol. Chem. 272*, 5616–5621.
38. Griffiths, J. R. (1979) Steady-state enzyme kinetics in mutual depletion systems. *Biochem. Soc. Trans. 7*, 429–439.

BI8006687